Density Functional Study on the Reaction Mechanism for the Reaction of Ni^+ with Ethane

ZHANG, Dong-Ju(张冬菊) **LIU, Cheng-Bu***(刘成卜) **LIU, Yong-Jun**(刘永军)
HU, Hai-Quan(胡海泉)
Institute of Theoretical Chemistry, Shandong University, Jinan, Shandong 250100, China

The mechanism of the reaction of Ni^+ (^2D) with ethane in the gas-phase was studied by using density functional theory. Both the B3LYP and BLYP functionals with standard all-electron basis sets are used to give the detailed information of the potential energy surface (PES) of $[Ni, C_2, H_6]^+$. The mechanisms forming the products CH_4 and H_2 in the reaction of Ni^+ with ethane are proposed. The reductive eliminations of CH_4 and H_2 are typical addition-elimination reactions. Each of the two reactions consists of two elementary steps: C—C or C—H bond activations to form inserted species followed by isomerizations to form product-like intermediate. The rate determining steps for the elimination reactions of forming CH_4 and H_2 are the isomerizations of the inserted species rather than C—C or C—H bond activations. The elimination reaction of forming H_2 was found to be thermodynamically favored compared to that of CH_4.

Keywords Ni^+, C_2H_6, reaction mechanism, density functional theory

Introduction

C—H and C—C bond activations of hydrocarbons by transition metal ions are of fundamental interest in various areas of chemical researches.[1,2] Many researches have shown that transition metal ions are able to activate the C—C and C—H bonds of saturated alkanes.[3-8] Experimentally, the intrinsic gas-phase properties of these ion-molecule reactions have been studied by using mass spectrometry techniques. Tonkyn and coworkers found that C_2H_6 could react with all first series transition metal ions except Mn^+ in 100 Pa of He, and the following reactions were observed [Eqs. (1—7)].[2,9]

$$M^+ + C_2H_6 \longrightarrow M(C_2H_4)^+ + H_2 \quad (1)$$

$$M^+ + C_2H_6 \longrightarrow MCH_2^+ + CH_4 \quad (2)$$

$$M^+ + C_2H_6 \longrightarrow MCH_3^+ + CH_3 \quad (3)$$

$$M^+ + C_2H_6 \longrightarrow MC_2H_2^+ + 2H_2 \quad (4)$$

$$M^+ + C_2H_6 \longrightarrow MH_2^+ + C_2H_4 \quad (5)$$

$$M^+ + C_2H_6 \longrightarrow MH^+ + C_2H_5 \quad (6)$$

$$M^+ + C_2H_6 \longrightarrow MH + C_2H_5^+ \quad (7)$$

where M^+ denotes a transition metal ion. For a given metal ion only some of the endothermic reactions could be observed in most cases. By inspecting the experimental results, these reactions can be rationalized in terms of the general mechanism depicted in Scheme 1.[2]

In this scheme, the metal ion first insert into a C—H or C—C bond via C—C or C—H bond activations, which lead to the formation of the intermediates **A** or **B**. The species **A** can further isomerize to **C** via β-H shift, which is a precursor for the elimination of H_2 together with the forming of the product **D**. In **C**, M^+ is inserted into H_2. Once **D** is formed, it can lead to the elimination of the second H_2 and the formation of product **E**. In order to explain the earlier experimental results and generalized mechanism postulated in Scheme 1 for

* E-mail: cbliu@sdu.edu.cn
Received May 28, 2001; revised September 12, 2001; accepted October 22, 2001.
Project supported by the National Natural Science Foundation of China (No. 20133020).

the reactions of the transitionm etal ions with ethane, a detailed theoretical study of these elementary step mechanisms is needed. It is well known that it is usually very difficult to theoretically calculate the electronic structure with accurate quantum mechanical methods, such as *ab initio* method for a system involving transition metals. As an alternative, density functional theory (DFT) has recently attracted considerable attention, which has been widely applied to electronic structure calculation for systems that contain transition metals and has been proven to be particularly effective in providing a wealth of information about molecular structure and energetics.[10-12]

Here, the reaction of Ni^+ with C_2H_6 as a prototype of the reactions of transition metal ions with ethane was chosen to study the elimination mechanism of CH_4 and H_2. So far as we know, a complete potential energy surface relevant to the reaction of Ni^+ with ethane has not been reported. Here, we report the explicit information on the structural and energetic details of all intermediates and transition states involved in this reaction. By using DFT method, all minimum and saddle points were located on the PES, and the details of reaction mechanisms for this reaction were shown. In this work our focus is on learning more details about the stationary points and saddle points on the PES for the $[Ni, C_2, H_6]^+$ cationic system, and the main aim is to give a qualitative model that explains how the M^+ activates the C—C and C—H bonds in alkanes. The theoretical predictions presented here for the reaction of Ni^+ with ethane can act as a guide for future comprehension of the reactions of transition metal ions with saturated alkanes.

Calculation details

The present DFT calculations were carried out by using Gaussian 98 programs.[13] Most of calculations were performed using Becke-3-LYP functional,[14] which is a hybrid functional including three fitted parameters and a mixture of Hartree-Fock exchange with DFT exchange-correlation. Although this functional is not very accurate,[15] it gives relatively good results for geometries, energies and bond dissociation energies of transition metal compounds.[16] So this functional has widely been used recently, especially for the systems involving transition metals. For Ni, the Wachters-Hay[17,18] all electron basis set extended with an *f* polarization function and a *d* diffuse function was used, which is scaled by factors of Raghavachari and Trucks.[19] For C and H, 6-31G* basis sets were used. In special calculations, the full geometry optimizations of the reactants, products, intermediates and transition states were performed at the selected theoretical level without imposing symmetry constraints. All the stationary points were positively identified for minima with no imaginary vibration frequencies and the transition states with one imaginary frequency. Corrections for zero-point energies have been taken into account. In order to verify the reliability of the information of the PES provided by us, all the geometries of the intermediates and transition states were also optimized by using BLYP functional at the same basis set mentioned above.

Scheme 1 Generalized mechanism for the reaction of transition metal ions M^+ with C_2H_4

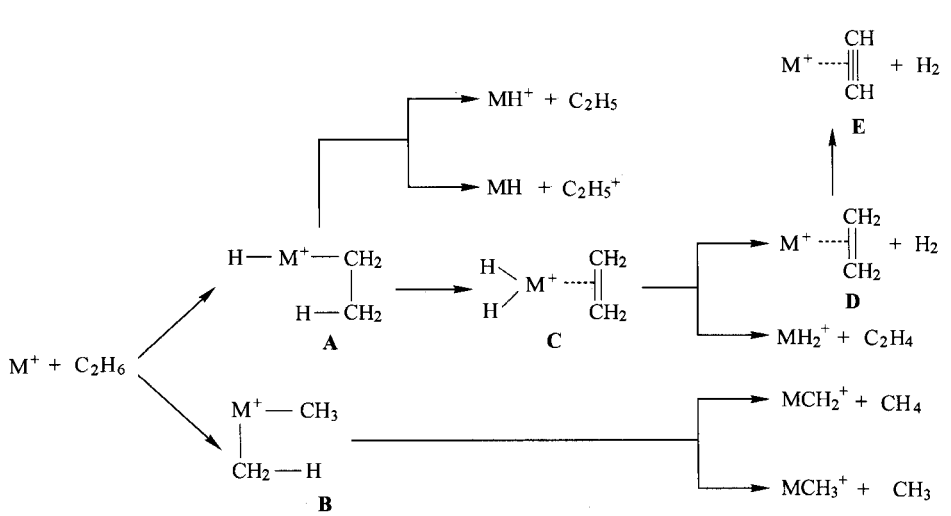

Results and discussion

The optimized structures of various species involved in the reaction of Ni^+ with ethane are shown in Figs. 1—3, respectively. The corresponding energies are listed in Table 1. The overall energetic profile for the reaction of Ni^+ with C_2H_6 is shown in Fig. 4. All processes designed here occur on the doublet state surface of $[Ni, C_2, H_6]^+$ since Ni^+ has a ^2D ($3d^9$) ground state. In Figs. 2 and 3, both the geometrical parameters of B3LYP and BLYP methods for various minima and first order saddle points involved with the $[Ni, C_2, H_6]^+$ system are shown. It is found that the geometrical parameters obtained using B3LYP functional are in good agreement with those obtained using BLYP functional, the spin contamination is small in all calculations, and the expectation values of $< S^2 >$ before projection are close to those of the corresponding pure spin state. Those values obtained using B3LYP method are shown in Table 1. From these facts, it can be concluded that the information on the PES $[Ni, C_2, H_6]^+$ given in the present work is correct, at least qualitatively. In the following discussions, only the results of B3LYP method for the sake of simplicity are discussed.

Five intermediates (**1**, **2**, **3**, **4** and **5**) and four first saddle points (**TS1**, **TS2**, **TS3** and **TS4**) on the PES were located. Intermediates **1** is an initial complex formed when Ni^+ (^2D) and C_2H_6 approach each other. **2** and **4** correspond to **A** and **B** postulated in Scheme 1, respectively. **3** and **5** are two product-like intermediates, which could directly lead to the eliminations of CH_4 and H_2, respectively. But intermediate **C** proposed in Scheme 1 was not found by using both B3LYP and BLYP methods. In intermediate **C**, Ni^+ has inserted into the H_2 bond. We use the inserted species as an initial geometry and attempt to locate a minimum on the PES, but the geometry optimizations always lead to either intermediate **4** or **5**. We also optimized its geometry using MP2 method and the basis set mentioned above, but it is unsuccessful again. It should be noted that **C**, the inserted species, is obviously different from **5**, which is a complex among H_2, Ni and C_2H_4 other than an inserted species. Thus, it can be concluded that **C** could not be a real minimum on the PES.

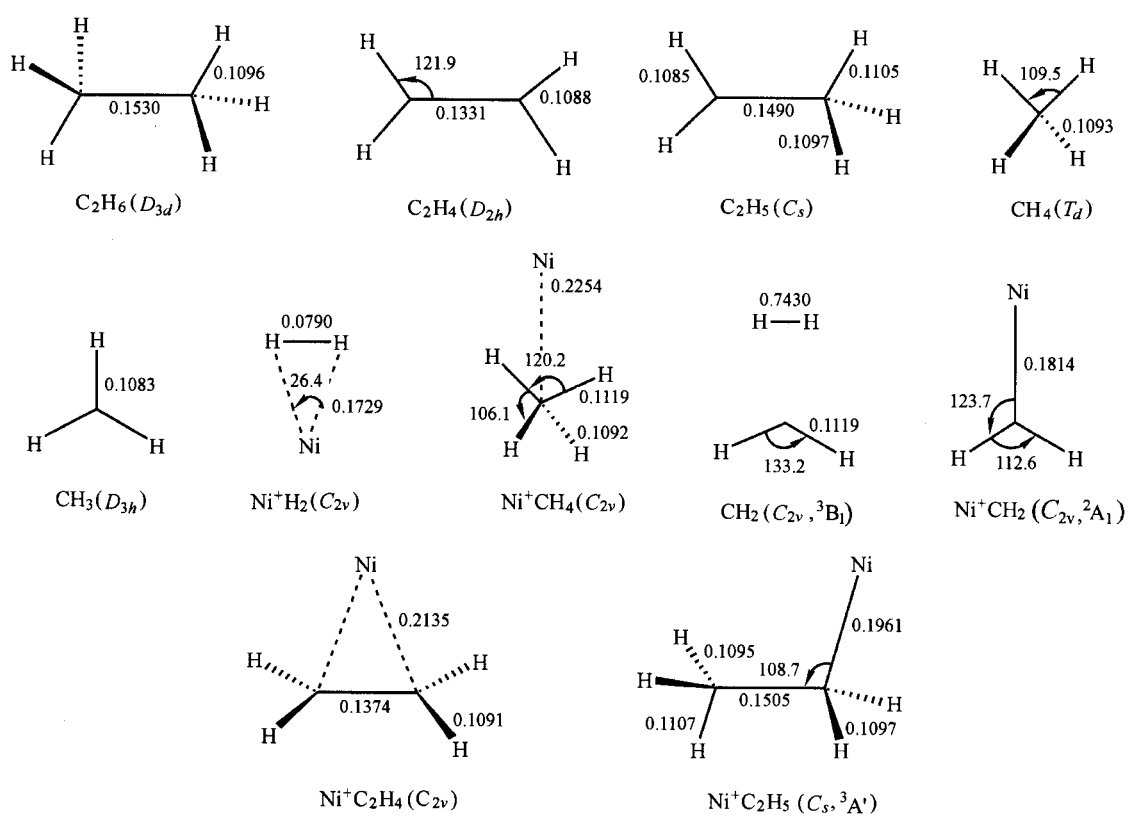

Fig. 1 Optimized geometries for the reactants and products of the reaction Ni^+ with C_2H_6 using B3LYP functional (in nm and degree).

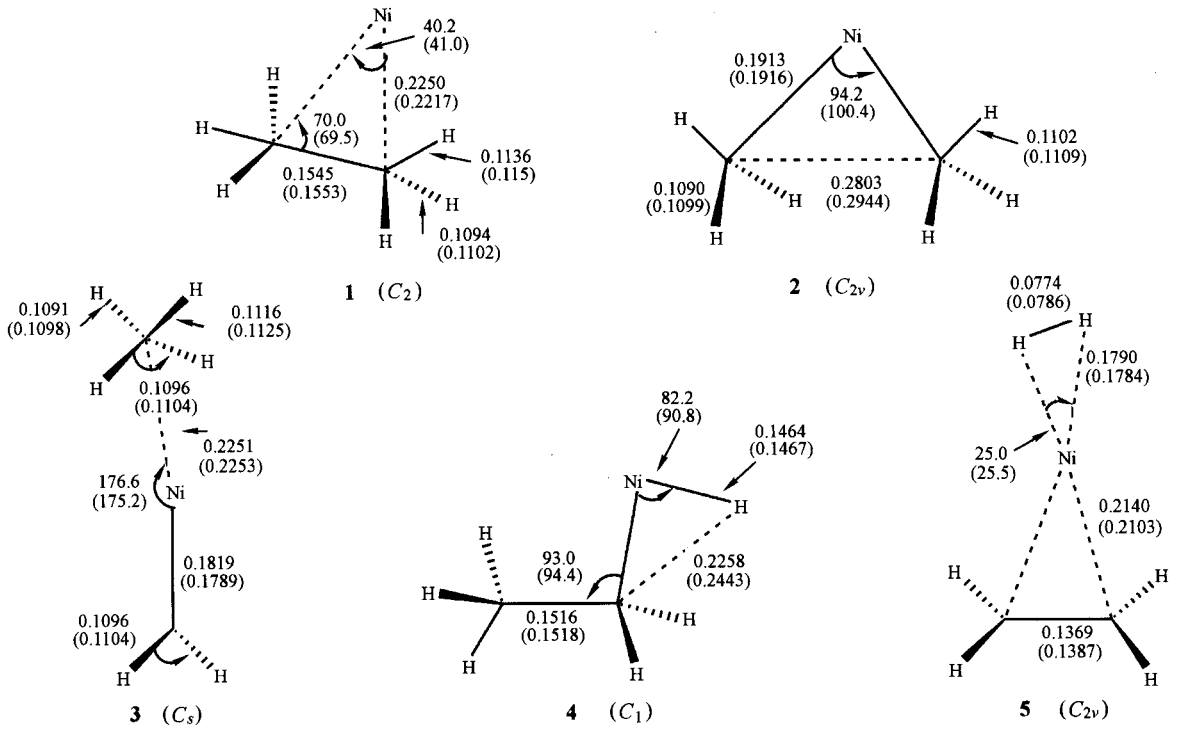

Fig. 2 Optimized geometrical parameters for the intermediates on the PES of $[Ni, C_2, H_4]^+$ with the results of B3LYP functional and of BLYP functional in parentheses (in nm and degree).

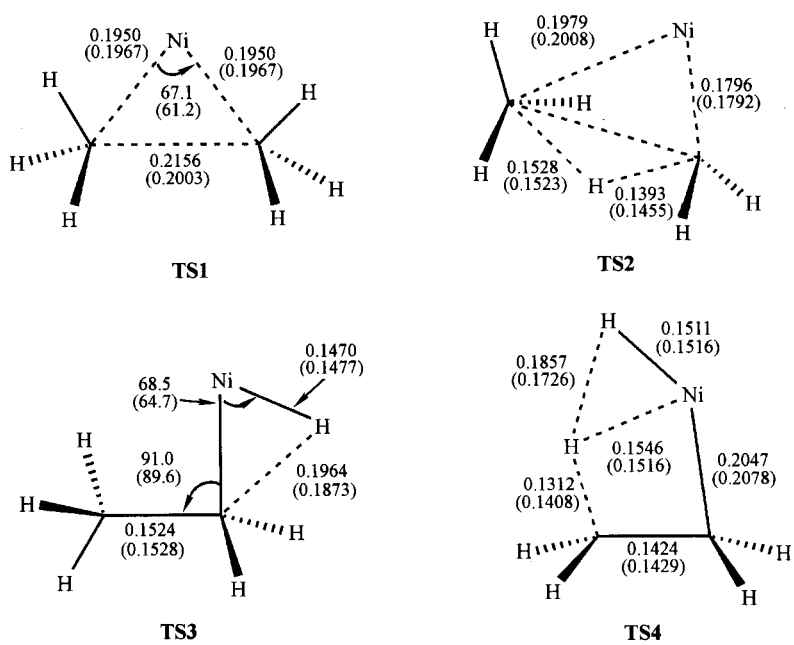

Fig. 3 Optimized geometries for the transition states on the PES of $[Ni, C_2, H_6]^+$ with the results of B3LYP functional and those of BLYP functional in parentheses (in nm and degree)

TS1 and **TS3** are the transition states of C—C and C—H bond activations, respectively, while **TS2** and **TS4** are H-shift transition states after Ni^+ inserting into C—C and C—H bonds, respectively. We find that **TS4**

bears some similarity to **C** proposed in Scheme 1. The intrinsic reaction coordinate (IRC) analysis shows that this transition state connects **4** and **5**, providing further evidence that **C** is not a real minimum on the PES.

Elimination mechanism of CH_4

As indicated in Fig. 4, a typical addition-elimination mechanism for the reaction of Ni^+ (^2D) with C_2H_6 is revealed. Our calculations show that both the elimination reactions of CH_4 and H_2 involve two elementary steps. One is the C—C or C—H bond activation to form the corresponding inserted intermediate and the other is the isomerization of the inserted species.

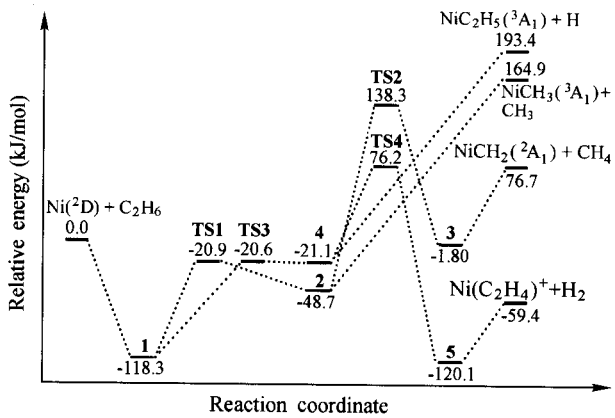

Fig. 4 Energetic profile for the reaction of Ni^+ with C_2H_6.

Table 1 Total and relative energies for optimized species[a]

Species	$< S^2 >$ [b,c]		Total energies	Relative energies	ZPE[c]
$Ni^+ + C_2H_6$	0.7514	0.0	−1587.714643	0.0	176.6
1	0.7547		−1587.759687	−118.3	197.2
2	0.7812		−1587.733180	−48.7	187.6
3	0.8877		−1587.715311	−1.80	183.3
4	0.7723		−1587.722667	−21.1	183.6
5	0.7527		−1587.760398	−120.1	178.2
TS1	0.7544		−1587.722599	−20.9	188.1
TS2	0.7826		−1587.661959	138.3	170.9
TS3	0.7635		−1587.722504	−20.6	182.8
TS4	0.7943		−1587.685618	76.2	172.9
$NiC_2H_4^+ + H_2$	0.7543	0.0	−1587.737269	−59.4	140.5, 26.7
$NiH_2^+ + C_2H_4$	0.7531	0.0	−1587.686401	74.1	35.0, 134.5
$NiC_2H_5^+ (^3A') + H$	2.0034	0.7500	−1587.640981	193.4	166.5
$NiH^+ (^3\Sigma_g) + C_2H_5$	2.0025	0.7539	−1587.609189	276.9	10.9, 156.6
$NiCH_2^+ (^2A_1) + CH_4$	0.8705	0.0	−1587.685440	76.7	59.2, 118.8
$NiCH_4^+ + CH_2 (^3B_1)$	0.7535	2.0052	−1587.596073	311.3	119.7, 45.7
$NiCH_3^+ (^3A_1) + CH_3$	2.0040	0.7538	−1587.651831	164.9	91.3, 78.3

[a] ZPE corrections have been taken into account, total energies are in hartree, and relative energies are in kJ/mol. [b] The expectation value of $< S^2 >$ before projection. Values after projection are 0.75 for double states and 2.00 for triplets. [c] The first number corresponds to the first species and the second number corresponds to the second species.

The elimination mechanism of CH_4 in the reaction was first analyzed. The initial electrostatic interaction between a Ni^+ with ethane leads to the formation of Ni-(C_2H_6)$^+$ adduct, intermediate **1**, which was found in C_2 symmetry. The geometry of this complex is similar to those of the ethane complex with Cu^+ and Co^+ given by Rosi[20] and Holthausen[21], respectively, but unlike those of the ethane complex with Cr^+, Fe^+ and Mo^+, which have C_s symmetry[20-22]. The formation of intermediate **1** is found to be a barrierless association. This adduct is predicted to be more stable than the Ni^+ (^2D) + C_2H_6 entrance channel by 118.3 kJ/mol. Ni—C distance in **1** is 0.2250 nm, and the lengths of C—C bond and two C—H bonds near to Ni are slightly longer than those in free C_2H_6. Since **1** is energy-rich and can rearrange to a dimethyl species **2** corresponding to **B** in Scheme 1, in

which the nickel has been inserted into the C—C bond. This inserted species has C_{2v} symmetry and its relative energy is computed to be 69.6 kJ/mol less stable than **1**, and to be 48.7 kJ/mol more stable than the entrance channel. **1** and **2** are connected by a saddle point, **TS1** with an activation barrier of 97.4 kJ/mol with respect to **1**. **TS1** is a three-member-ring transition state and has C_1 symmetry. The breaking C—C bond is elongated to 0.2156 nm and the forming Ni—C bond is shortened to 0.1950 nm. This saddle point bears similarity to **2**, which occurs very "late" on the PES. The imaginary frequency of the saddle point is 375i cm^{-1}, and the corresponding transition vector indicated by the vibration analysis corresponds to the breaking of the C—C bond and the reorientation of the methyl groups. The relative energy of this saddle point is 20.9 kJ /mol below the energy of the separated reactants.

Once **2** is formed, it can undergo two possible production channels immediately by isomerization or decomposition. One is the process directly cleaving Ni—C bond in **2**, which leads to $NiCH_3^+ + CH_3\cdot$ as proposed in scheme 1. The process is endothermic by 164.9 kJ/mol. The other is an energetically more favorable reaction path, which involves the isomerization of **2** into **3** via a three-center transition state **TS2**. As shown in Fig. 3, **TS2** is a H-migration transition state on the PES, in which a H atom moves from a C atom to the other C atom and the breaking and forming C—H bond lengthes are 0.1393 nm and 0.1528 nm, respectively. The corresponding imaginary frequency is 1300i cm^{-1}. The vibration analyses have also shown that the corresponding transition vectors are completely consistent with the notion of a 1,3-H shift. It is very obvious from Fig. 4 that the energy of **TS2** is much higher than that of **TS1**, and its relative energy is 138.3 kJ/mol above the entrance channel. So the second step relevant to this rearrangement process along the CH_4 elimination path is the rate-determining step. The barrier height from **2** to **TS2** is 187.0 kJ/mol, which is higher as compared to the C—C bond activation process, a barrier of 97.4 kJ/mol. **3** is a complex between CH_4 and $NiCH_2^+$, which has a C_s symmetry. Both the methane moiety and the nickel-carbene unit in **3** are only slightly distorted compared to the geometric parameters of the free CH_4 and $NiCH_2^+$, respectively. **3** is computed to be 1.80 kJ/mol below the energy of the separated reactants. After species **3** is formed, the production channel of dissociating into $NiCH_2^+ (^1A) + CH_4$ would be open, which requires 78.5 kJ/mol, and the overall reaction $Ni^+ (^2D) + C_2H_6 \rightarrow NiCH_2^+ (^1A) + CH_4$ is endothermic by 76.7 kJ/mol. The other exit channel, **3** breaking up into $Ni(CH_4)^+ + CH_2$, requires 311.3 kJ/mol and should be much less favorable energetically.

Elimination mechanism of H_2

Now the other reaction paths on the PES of $[Ni, C_2, H_6]^+$ are studied, which involves the elimination of H_2.

This elimination channel of H_2 also consists of two elementary steps. From Fig. 4, it can be found that the initial $Ni(C_2H_6)^+$ complex **1** can also be converted into **4**, a C—H bond inserted species, via a C—H cleavage transition state **TS3**. It should be noted that in both **4** and **TS3** the longest C—H bond in methyl group is located in a *trans* arrangement for H-C-C-Ni. Their geometries obtained in the present work differ significantly from those on the PES of $[Co, C_2, H_6]^+$ and $[Co, C_2, H_6]^+$ found by Holthausen *et al.*[21,22] The most favorable geometry of the C—H inserted intermediate and corresponding C—H activation transition state are a *cis* arrangement for H-C-C-M, where M denotes Co and Fe. But in our calculations, the *cis* geometries are not the minima on the PES of $[Ni, C_2, H_6]^+$. This C—H bond inserted species is calculated to be 27.6 kJ/mol less stable compared to the C—C bond inserted species, **2**. The barrier height for this channel is 97.7 kJ/mol relative to **1**. **TS3** has C_1 symmetry, and the transition vector associated with the imaginary frequency of 756i cm^{-1} confirms **TS3** as the correct saddle point for the C—H bond insertion reaction. The breaking C—H bond is elongated to 0.1964 nm in **TS3**. The structure of this transition state bares already large similarity to **4**, and indicates that **TS3** is very loose. As a result, the energy of **TS3** is only 0.5 kJ/mol above the **4**. It is also found that the energy of **TS3**, the C—H bond cleavage transition state, is only higher by 0.3 kJ/mol than that of **TS1**, the C—C bond cleavage transition state. Thus, from a pure energetical point of view, both the C—C and C—H bond activation pathways have almost equal probability.

Proceeding further along the reaction coordinate, the C—H inserted species **4**, can either undergo direct

bond cleavages leading to $NiC_2H_5^+$ (^1A) + H· or NiH^+ ($^3\Sigma_g$) + C_2H_5·, computed to be endothermic by 193.4 and 276.9 kJ/mol with respect to Ni^+ (^2D) + C_2H_6, or rearrange into a rather stable complex **5**, energetically located 120.1 kJ/mol below the entrance channel. **4** and **5** are connected by a saddle point **TS4**. This transition structure has an imaginary frequency of 688i cm^{-1}. Just as shown in Fig. 3, it is a four-center transition state. This structure bears some semblance to C proposed in Scheme 1. In **TS4**, the breaking C—H bond length is 0.1312 nm, and the distances between Ni^+ and two H atoms are 0.1511 and 0.1546 nm, respectively. The height of the activation barrier amounts to 76.2 kJ/mol with respect to the entrance channel. Relative to **4**, the barrier is 97.3 kJ/mol. Thus, it is very obvious that the energetic bottleneck is the second step in the reaction path of H_2 elimination, similar to the situation of CH_4 elimination. **5** is a product-like complex among H_2, Ni^+ and C_2H_4. Both minima, it can break up by expulsion of either molecular hydrogen together with $Ni(C_2H_4)^+$ and product **D** proposed in Scheme 1 or ethylene with NiH_2^+. The overall reaction Ni^+ (^2D) + $C_2H_6 \rightarrow NiC_2H_4^+ + H_2$ is exothermic by 59.4 kJ/mol, while the process corresponding to Ni^+ (^2D) + $C_2H_6 \rightarrow NiH_2^+ + C_2H_4$ is less favorable with high relative energy of 76.74 kJ/mol above the entrance channel.

Conclusions

The structural and energetic details of $[Ni, C_2, H_6]^+$ have been investigated by employing DFT. The following conclusions can be drawn from our theoretical calculations.

(1) The typical addition-elimination mechanism was revealed for the reaction of Ni^+ (^2D) with C_2H_6, and the mechanistic details on the eliminations of CH_4 and H_2 for the reaction of $Ni^+ + C_2H_6$ were given.

(2) Both the CH_4 and H_2 elimination channels undergo two elementary steps. The first steps are that Ni^+ inserts into C—C or C—H bonds, respectively, then the rearrangements of the inserted-intermediate lead to the elimination of CH_4 and H_2, which are the rate-determining steps.

(3) The first-order saddle points **TS1** and **TS3**, which lead to Ni^+ inserting into C—C bond and C—H bond, respectively, are energetically located close. From a kinetic point of view, two main reaction channels should compete along the reaction coordinate and have almost equal probability. But it seems that the CH_4 elimination reaction is thermodynamically disfavored as compared to the C—H bond activation, since the activation energy of the second step of this reaction is higher than that of H_2 elimination reaction.

References

1 Haggin, J. *Chem. Eng. News* **1993**, *71*, 27.
2 Eller, K.; Schwarz, H. *Chem. Rev.* **1991**, *91*, 1121 and references therein.
3 Weisshaar, J. C. *Acc. Chem. Res.* **1993**, *26*, 213.
4 Schultz, R. H.; Elkind, J. L.; Armentrout, P. B. *J. Am. Chem. Soc.* **1988**, *110*, 411.
5 Tonkyn, R.; Ronan, M.; Weisshaar, J. C. *J. Phys. Chem.* **1988**, *92*, 92.
6 Schulze, C.; Schwarz, H.; Peake, D. A.; Gross, M. L. *J. Am. Chem. Soc.* **1987**, *109*, 2368.
7 van Koppen, P. A. M.; Brodbelt-Lustig, J.; Bowers, M. T.; Dearden, D. V. *J. Am. Chem. Soc.* **1991**, *113*, 2359.
8 van Koppen, P. A. M.; Bowers, M. T.; Fisher, E. R.; Armentrout, P. B. *J. Am. Chem. Soc.* **1994**, *116*, 3780.
9 Tonkyn, R; Ronan, M.; Weisshaar, J. C. *J. Phys. Chem.* **1988**, *92*, 92 and references therein.
10 Can Daelen, M. A.; Li, Y. S.; Newsam, J. M.; van Santen, R. A. *J. Phys. Chem.* **1996**, *100*, 2279.
11 Ziegler, T. *Chem. Rev.* **1991**, *91*, 651.
12 Cheng, H.; Reiser, D. B.; Mathis, P. M.; Baumert, K; Dean, S. W., Jr. *J. Phys. Chem.* **1996**, *100*, 9800.
13 Gaussian 98, Gaussian Inc., Pittsburgh, PA, **1998**.
14 Becke, A. D. *J. Chem. Phys.* **1993**, *98*, 5648.
15 Kais, S.; Herschbach, N. C. H.; Murry, C. W.; Frish, G. J. *J. Chem. Phys.* **1993**, *99*, 417.
16 Siegbahn, P. E. M. *Adv. Chem. Phys.* **1996**, *XCIII*, 333.
17 Wachters, A. J. H. *J. Chem. Phys.* **1970**, *52*, 1033.
18 Hay, P. J. *J. Chem. Phys.* **1977**, *66*, 4377.
19 Raghavachari, K.; Trucks, G. W. *J. Chem. Phys.* **1989**, 91, 1062.
20 Rosi, M.; Bauschlicher, C. W., Jr.; Langhoff, S. R. *J. Phys. Chem.* **1990**, *94*, 8656.
21 Holthausen, M. C.; Koch, W. *J. Am. Chem. Soc.* **1996**, *118*, 9932.
22 Holthausen, M. C.; Fiedler, A.; Schwarrz, H.; Koch, W. *J. Phys. Chem.* **1996**, *100*, 6236.

(E0105283 LI, L. T.; DONG, L. J.)